



**Annalise CXR**  
**Product Version: 2.1**  
**Date of Issue: 2021-06-03**

**Annalise CXR Performance Guide**  
English

*Manufacturer*



**ANNALISE-AI PTY LTD**

ACN 635 645 260

Level 5, 24 York Street

Sydney NSW 2000,

Australia

Copyright © annalise-AI Pty Ltd, 2021



## 1. Performance

This document provides product performance information pertaining to Annalise CXR. For general user information please refer to the User Guide.

The following table includes all supported findings for Annalise CXR, presented in alphabetical order. Each row shows the finding name and the AUC.

These performance results are based on the data set that Annalise.ai has used to evaluate the product. Differences in demographics, imaging equipment or other variables may result in changes in performance.

## 2. AUC by Findings

| Finding                         | AUC mean |
|---------------------------------|----------|
| Abdominal clips                 | 0.9778   |
| Acute clavicle fracture         | 0.9603   |
| Acute humerus fracture          | 0.9740   |
| Acute rib fracture              | 0.9688   |
| Airway stent                    | 0.9664   |
| Aortic arch calcification       | 0.9759   |
| Aortic stent                    | 0.9942   |
| Atelectasis                     | 0.8825   |
| Axillary clips                  | 0.9964   |
| Basal interstitial thickening   | 0.8870   |
| Biliary stent                   | 0.9994   |
| Breast implant                  | 0.9963   |
| Bronchiectasis                  | 0.9282   |
| Diffuse bullae                  | 0.9686   |
| Lower zone bullae               | 0.9534   |
| Upper zone bullae               | 0.9636   |
| Calcified axillary nodes        | 0.9777   |
| Calcified granuloma (< 5mm)     | 0.9303   |
| Calcified hilar lymphadenopathy | 0.8913   |
| Calcified mass (> 5mm)          | 0.9534   |
| Calcified neck nodes            | 0.9327   |
| Calcified pleural plaques       | 0.9800   |
| Cardiac valve prosthesis        | 0.9973   |
| Cavitating mass with content    | 0.9712   |
| Cavitating mass(es)             | 0.9285   |
| Cervical flexion                | 0.9920   |
| Incompletely imaged chest       | 0.9814   |
| Chronic clavicle fracture       | 0.9624   |
| Chronic rib fracture            | 0.9480   |

|   |        |
|---|--------|
| Chronic humerus fracture                      | 0.9878 |
| Clavicle fixation                             | 0.9973 |
| Clavicle lesion                               | 0.9659 |
| Coronary stent                                | 0.9663 |
| Diaphragmatic elevation                       | 0.9332 |
| Diaphragmatic eventration                     | 0.9825 |
| Diffuse airspace opacity                      | 0.9787 |
| Diffuse fibrotic volume loss                  | 0.9603 |
| Diffuse interstitial thickening               | 0.9380 |
| Diffuse lower airspace opacity                | 0.9334 |
| Diffuse nodular / miliary lesions             | 0.9793 |
| Diffuse pleural thickening                    | 0.9630 |
| Diffuse spinal osteophytes                    | 0.9871 |
| Diffuse upper airspace opacity                | 0.9773 |
| Distended bowel                               | 0.9792 |
| Electronic cardiac devices                    | 0.9999 |
| Focal airspace opacity                        | 0.8508 |
| Gallstones                                    | 0.8705 |
| Gastric band                                  | 0.9748 |
| Hiatus hernia                                 | 0.9914 |
| Hilar lymphadenopathy                         | 0.9363 |
| Humeral lesion                                | 0.9753 |
| Hyperinflation                                | 0.9643 |
| Image obscured                                | 0.9377 |
| In position Central Line (CVC)                | 0.9951 |
| In position Endotracheal Tube (ETT)           | 0.9971 |
| In position Nasogastric Tube (NGT)            | 0.9966 |
| In position Pulmonary Arterial Catheter (PAC) | 0.9924 |
| Inferior mediastinal mass                     | 0.9687 |
| Intercostal drain                             | 0.9965 |
| Internal foreign body                         | 0.9328 |
| Kyphosis                                      | 0.9761 |
| Loculated effusion                            | 0.9525 |
| Lower zone fibrotic volume loss               | 0.9226 |
| Lung collapse                                 | 0.9971 |
| Lung sutures                                  | 0.9658 |
| Mastectomy                                    | 0.9615 |
| Mediastinal clips                             | 0.9930 |
| Multifocal airspace opacity                   | 0.8954 |
| Multiple masses or nodules                    | 0.9565 |
| Neck clips                                    | 0.9867 |
| Nipple shadow                                 | 0.9712 |

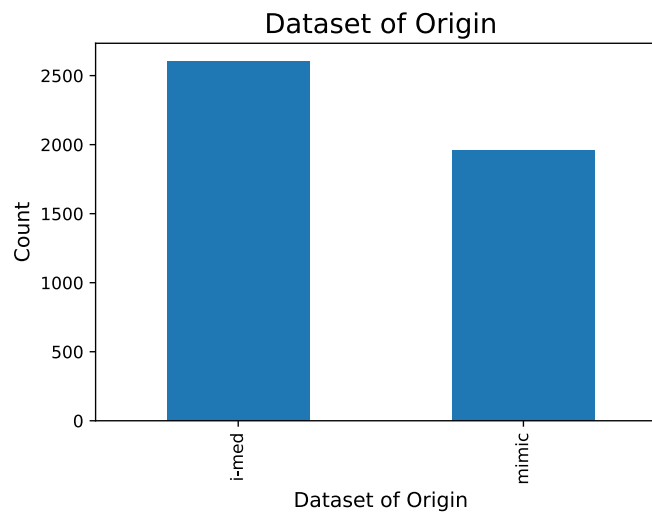
|                                    |        |
|------------------------------------|--------|
| Oesophageal stent                  | 0.9980 |
| Osteopaenia                        | 0.9551 |
| Overexposed                        | 0.9162 |
| Patient rotation                   | 0.9100 |
| Pectus carinatum                   | 0.9000 |
| Pectus excavatum                   | 0.9936 |
| Peribronchial cuffing              | 0.8357 |
| Pericardial fat pad                | 0.9251 |
| Perihilar airspace opacity         | 0.9430 |
| Pleural mass                       | 0.9483 |
| Pneumomediastinum                  | 0.9689 |
| Post resection volume loss         | 0.9795 |
| Pulmonary artery enlargement       | 0.9420 |
| Pulmonary congestion               | 0.9256 |
| Reduced lung markings              | 0.9544 |
| Rib fixation                       | 0.9908 |
| Rib lesion                         | 0.9708 |
| Rib resection                      | 0.9860 |
| Rotator cuff anchor                | 0.9996 |
| Scapular fracture                  | 0.9424 |
| Scapular lesion                    | 0.9518 |
| Scoliosis                          | 0.9547 |
| Segmental collapse                 | 0.9111 |
| Shoulder arthritis                 | 0.9829 |
| Shoulder dislocation               | 0.9664 |
| Shoulder fixation                  | 0.9969 |
| Shoulder replacement               | 1.0000 |
| Simple effusion                    | 0.9513 |
| Simple pneumothorax                | 0.9804 |
| Solitary lung mass                 | 0.9455 |
| Solitary lung nodule               | 0.8978 |
| Spinal fixation                    | 0.9993 |
| Spinal arthritis                   | 0.9378 |
| Spinal lesion                      | 0.9708 |
| Spinal wedge fracture              | 0.9673 |
| Sternotomy wires                   | 0.9999 |
| Subcutaneous emphysema             | 0.9964 |
| Subdiaphragmatic gas               | 0.9958 |
| Suboptimal Central Line (CVC)      | 0.9755 |
| Suboptimal Endotracheal Tube (ETT) | 0.9947 |
| Suboptimal gastric band            | 0.9967 |
| Suboptimal Nasogastric Tube (NGT)  | 0.9847 |

|  |        |
|--|--------|
| Suboptimal Pulmonary Arterial Catheter (PAC) | 0.9933 |
| Superior mediastinal mass                    | 0.9520 |
| Tension pneumothorax                         | 0.9973 |
| Tracheal deviation                           | 0.9512 |
| Underexposed                                 | 0.9463 |
| Underinflation                               | 0.9725 |
| Unfolded aorta                               | 0.8956 |
| Upper interstitial thickening                | 0.8995 |
| Upper zone fibrotic volume loss              | 0.9764 |
| Widened aortic contour                       | 0.9812 |
| Widened cardiac silhouette                   | 0.9510 |

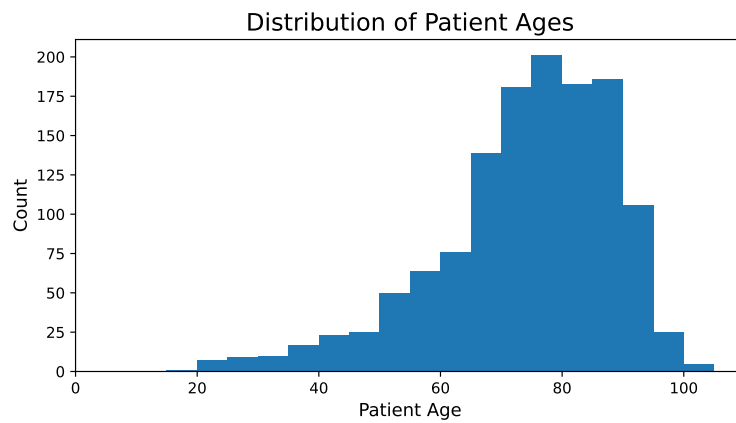
### 3. Model Validation Dataset Characteristics

The Annalise CXR product is validated on over 2,500 studies acquired from clinics across Australia and the United States of America.

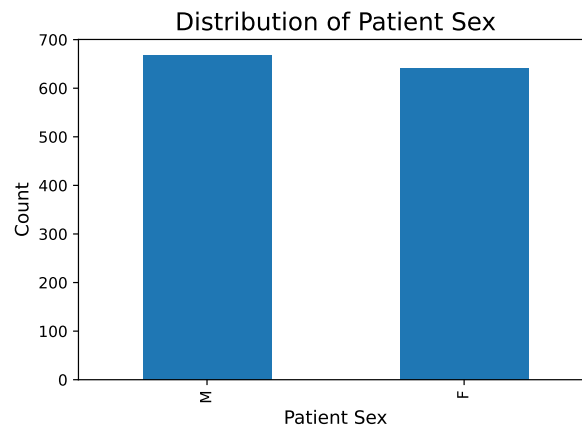
#### 3.1 Dataset of Origin of images:



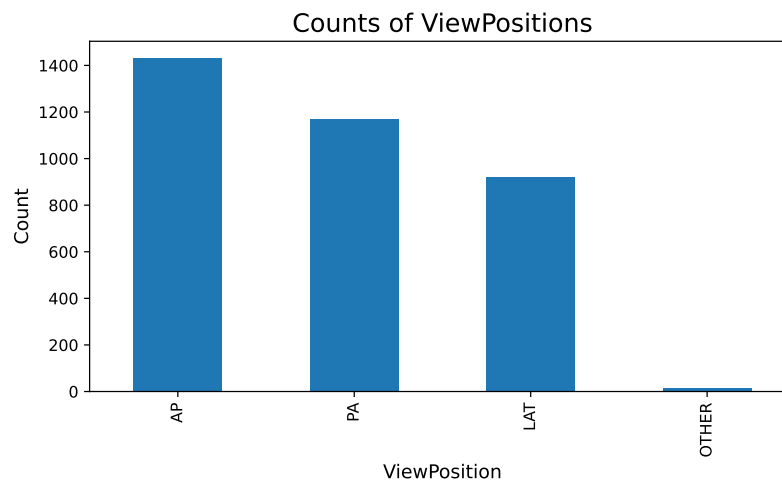
### 3.2 Patient Age



### 3.3 Patient Sex

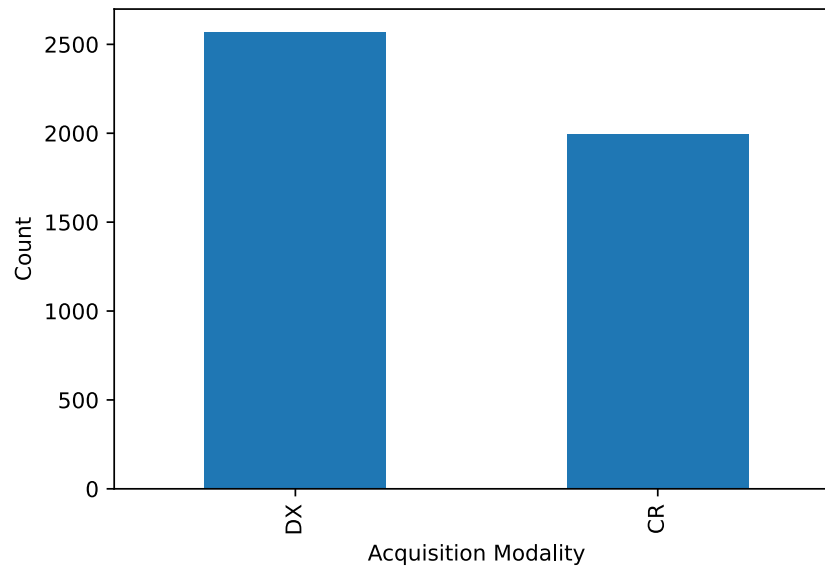


### 3.4 ViewPosition Characteristics



#### 4. Acquisition Modality of Images

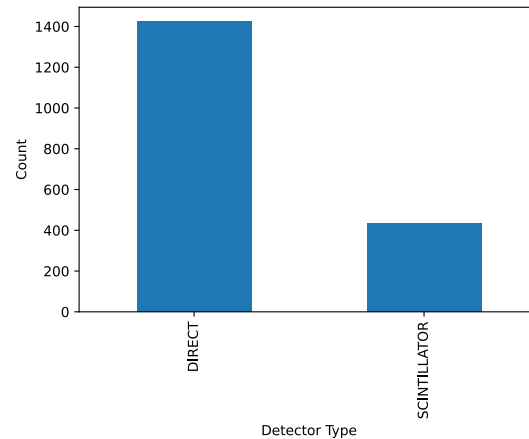
The Acquisition Modality is an important marker of image quality. Computed Radiography (CR) is an older technology which records information on a phosphor cassette prior to digitization while Digital Radiography (DX) records and digitizes information at the detector, leading to improved spatial resolution. Decreased spatial resolution may lead to difficulty in distinguishing fine detail on X-rays such as rib fractures or lung nodules.



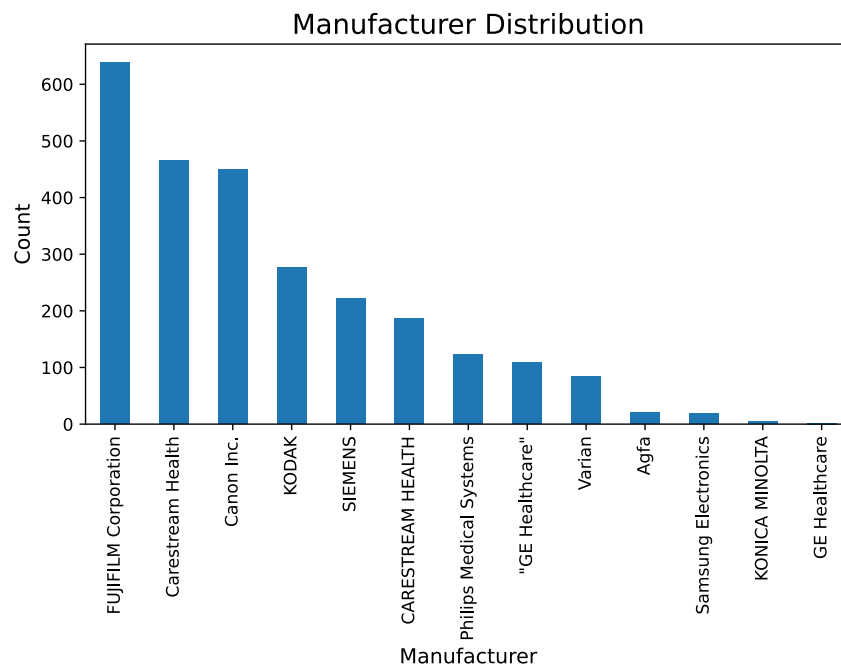


## 5. Detector Type

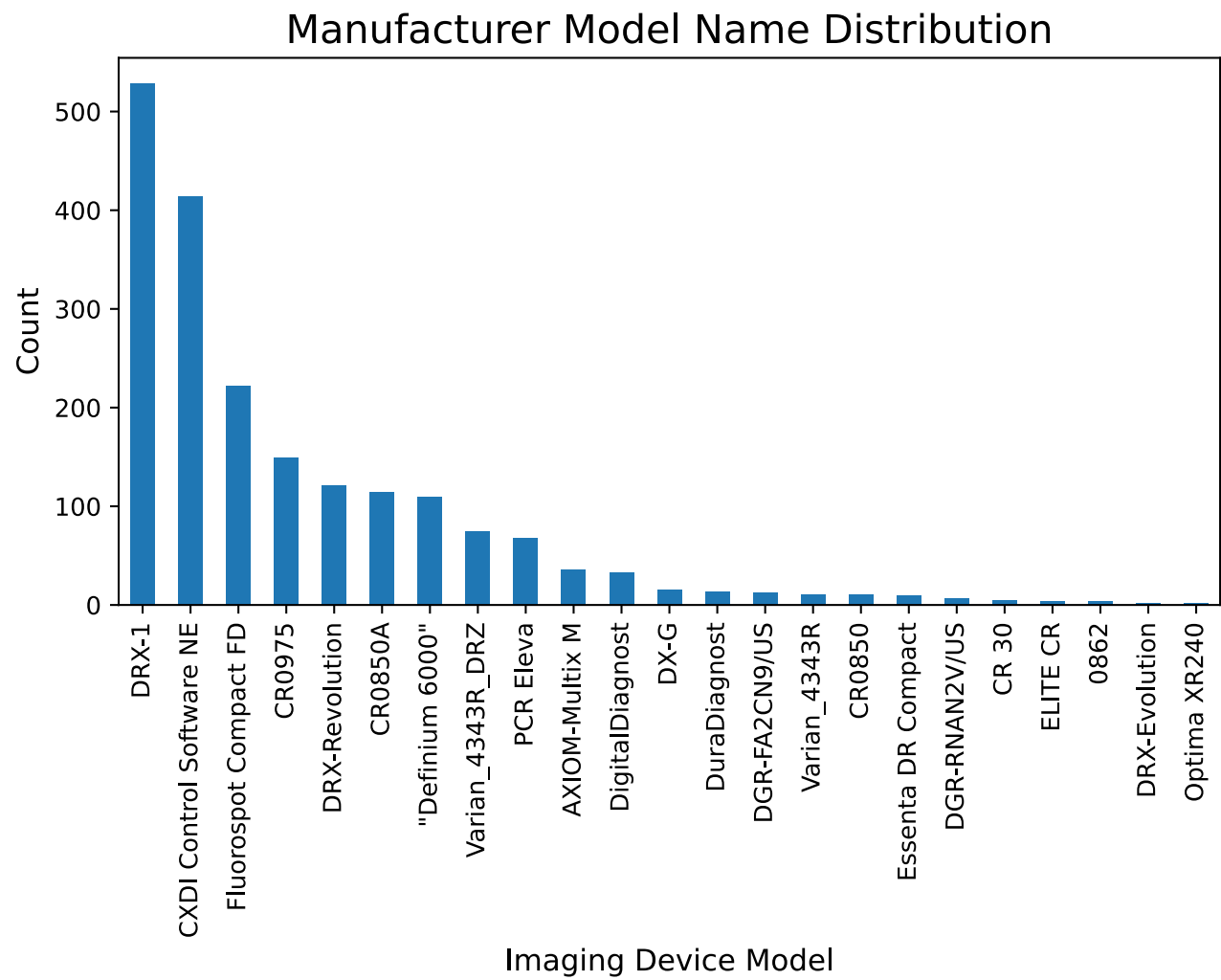
When Digital Radiography is used, the type of detector also changes the image quality. Scintillator detectors are older technologies which convert X-ray photons to visible photons via scintillation crystals while Direct detectors detect X-ray photons without an intermediate step. Direct detectors tend to have improved modulation transfer function and spatial resolution. Decreased spatial resolution may lead to difficulty in distinguishing fine detail on X-rays such as rib fractures or lung nodules.



## 6. Imaging Device Manufacturers



## 7. Imaging Device Model

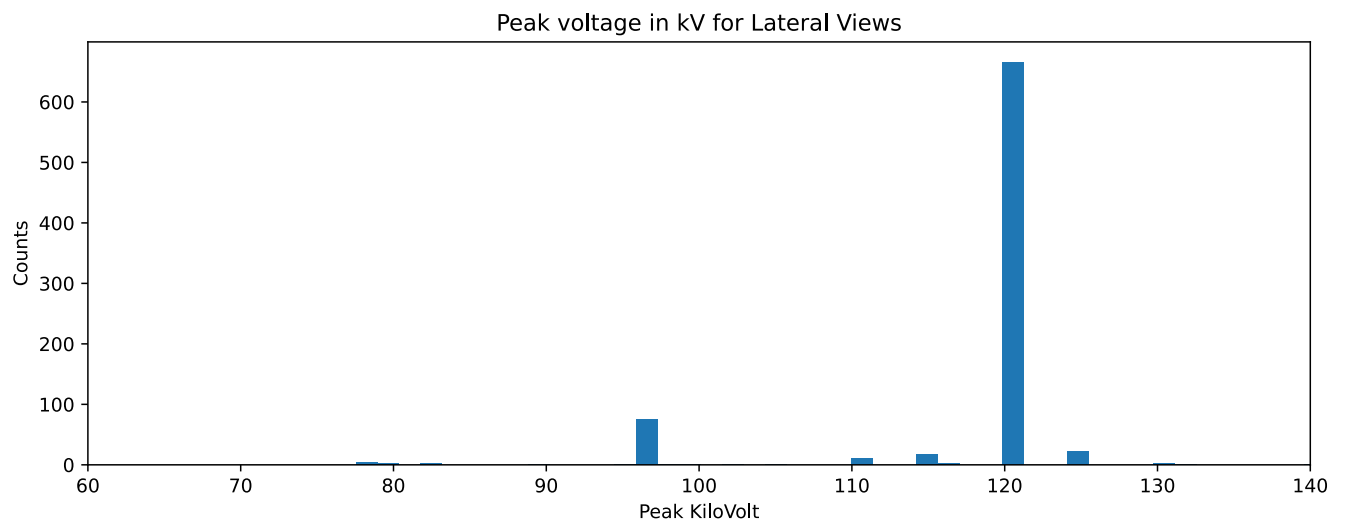
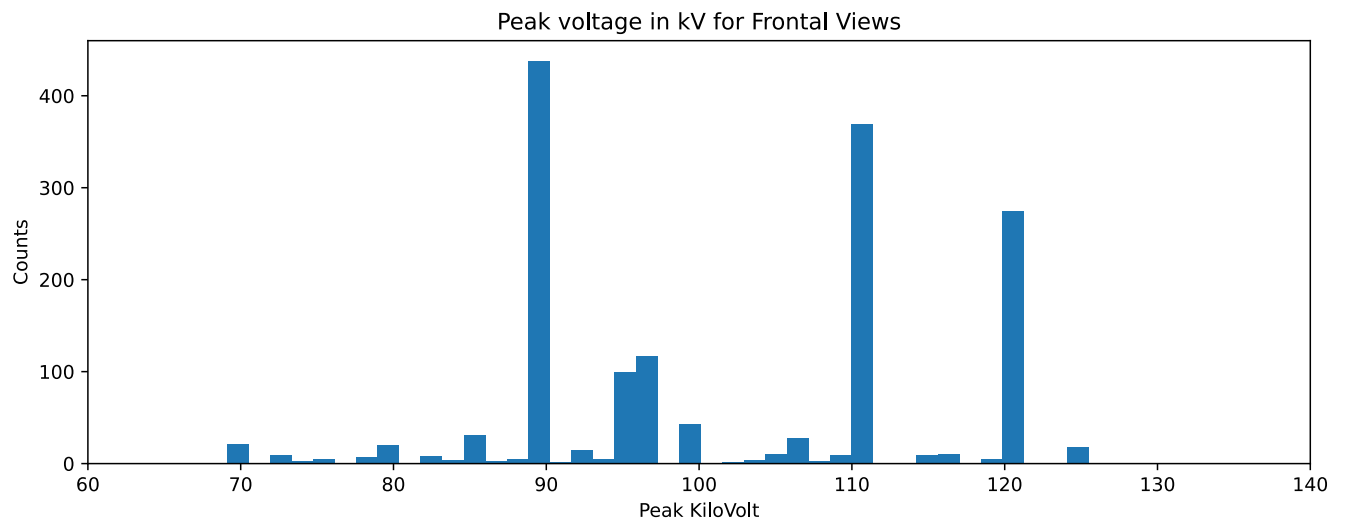


## 8. Distribution of Peak kV

The Peak KV is selected by the radiographer at the time of imaging and can affect image quality.

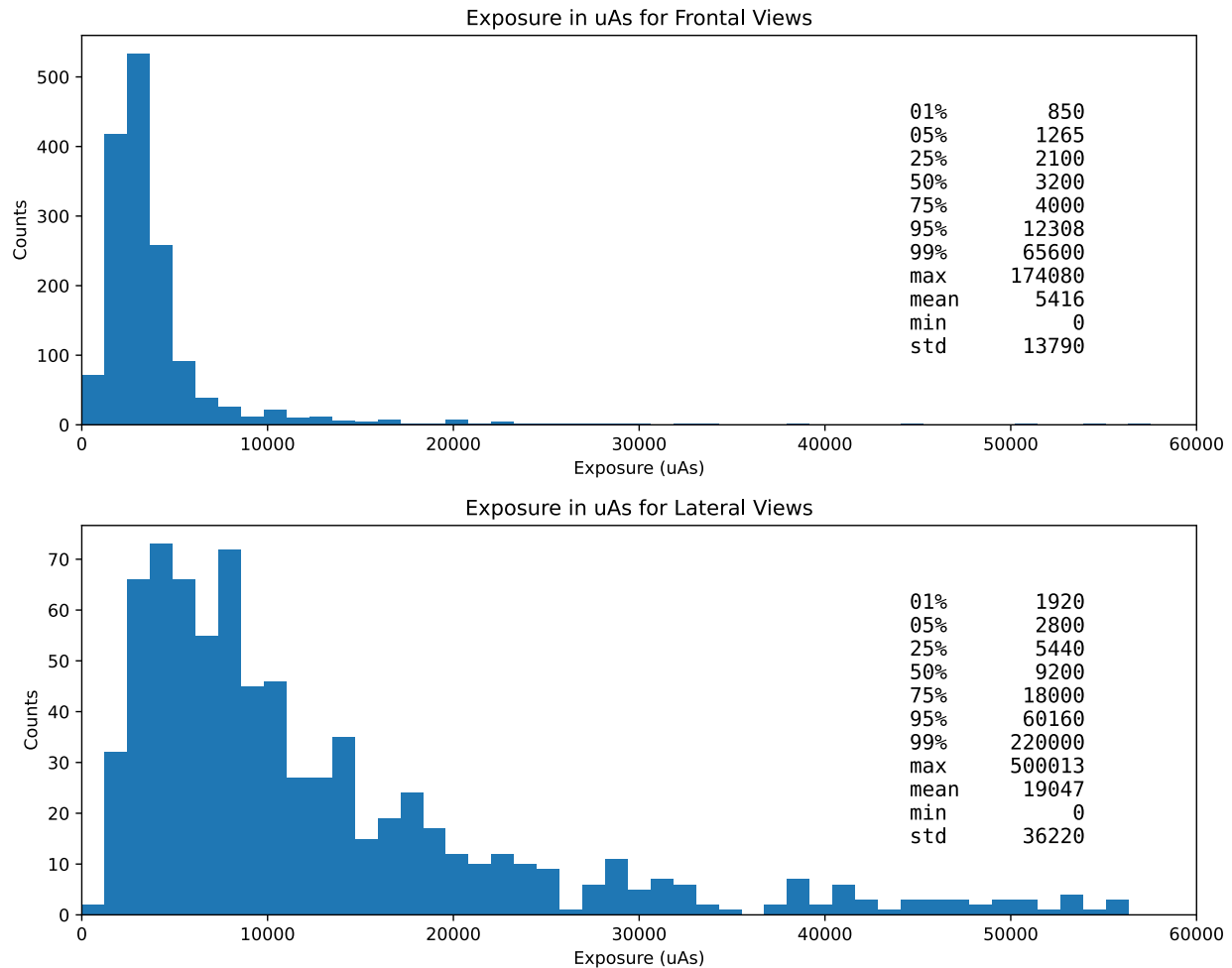
With automatic exposure control in most systems, higher KVP leads to more x-rays passing through the body and reaching the detector, reducing dose but also reducing contrast resolution.

Lower KVP improves contrast resolution but increases dose to the patient. Too high KVP may lead to difficulty in distinguishing low contrast structures like lung opacities.



## 9. Distribution of Exposure in uAs

The exposure in micro-ampere-seconds is the total output of the X-ray tube and is usually automatically controlled through the use of Automatic Exposure Control, which aims to maintain image quality while reducing exposure as low as reasonably achievable. Hence, lateral views where there is more tissue for the X-ray photons to pass through will require more exposure. Changing the exposure manually will change the Exposure Index and Deviation Index

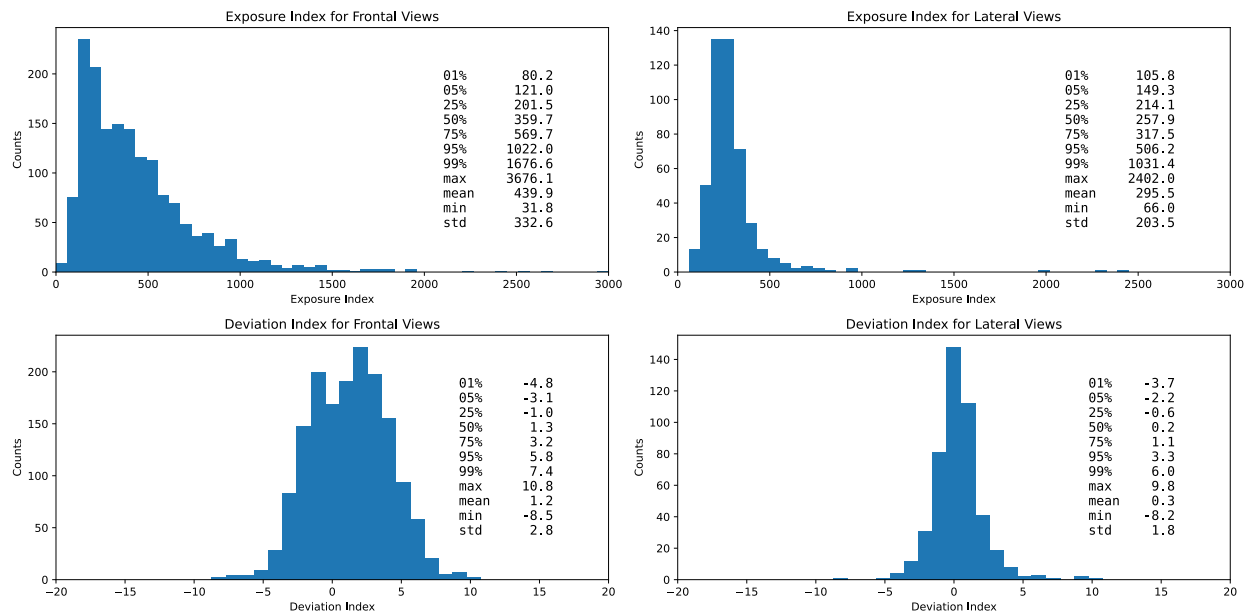


## 10. Radiograph Quality Indices

The exposure index is a measure of the incident radiation on the detector plate. When automatic exposure control is used, this should be roughly similar within the same exam type (e.g. frontal chest radiographs) as AEC aims to maintain exposure at a target exposure index

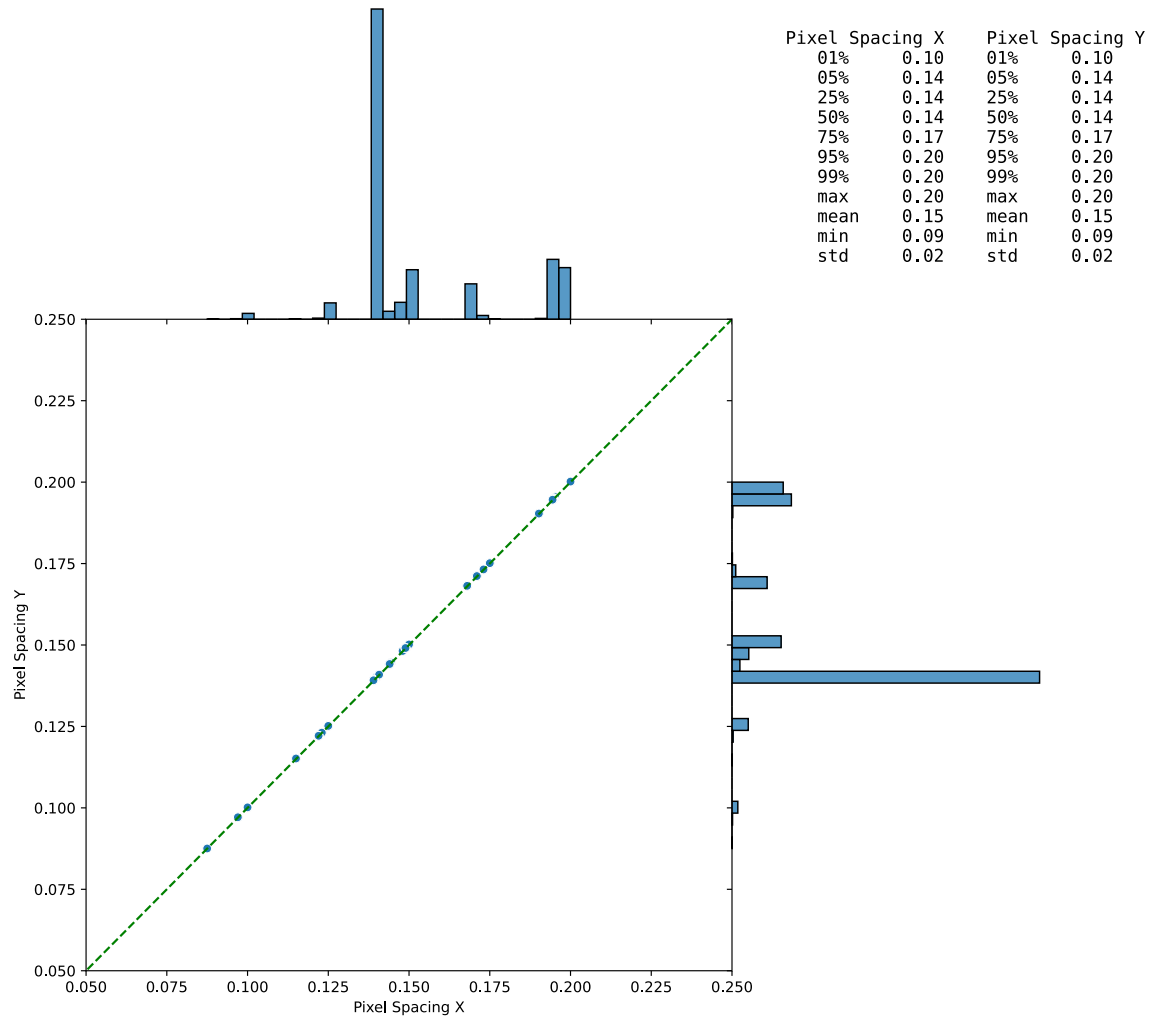
The deviation index is a logarithmic measure of the difference between the target exposure index and the actual target exposure. High deviation index indicates overexposure while low deviation index indicates underexposure (likely to cause the image to appear more white than necessary)

Different EIs and DIs may lead to difficulty in visualizing structures with poor contrast resolution such as lung opacities.



## 11. Pixel Spacing Values

Pixel spacing is the measure of the physical distance between each recorded pixel on the detector. It is not adjusted for geometric magnification. Higher pixel spacing values typically indicate improved spatial resolution unless post-processing has been applied to the image. Decreased spatial resolution may lead to difficulty in distinguishing fine detail on X-rays such as rib fractures or lung nodules.



△ annalise.ai

△ annalise.ai

Annalise-AI Pty Ltd,  
Level 5,  
24 York Street,  
Sydney, NSW 2000, Australia

ABN: 92 635 645 260

Annalise-AI UK  
Ltd, 100 New  
Bridge Street,  
London,  
EC4V 6JA,  
England

Company no: 12804340

[support@annalise.ai](mailto:support@annalise.ai)

[www.annalise.ai](http://www.annalise.ai)

OPT-PRM-006 V2